'ndian J. Phys. 78A (3), 367-375 (2004)

AN INTERNATIONAL JOURNAL
IJP A

Particular solutions of GLDAP evolution equations in leading order and structure functions at low-x

R Rajkhowa and J K Sarma*
Department of Physics, Tezpur University, Napaam,
Tezpur-784 028, Assam, India
E-mail : jks@tezu.ernet.in

Received 26 June 2003, accepted 3 November 2003

Abstract : We present particular solutions of singlet and non-singlet Gribov-Lipatov-Dokshitzer-Altarelli-Parisi (GLDAP) evolution equations in leading order (LO) at low-x. We obtain t-evolutions of proton and neutron structure functions and x-evolutions of deuteron structure functions at low-x from GLDAP evolution equations. The results of t-evolutions are compared with HERA low-x and low-Q^2 data and those of x-evolutions are compared with NMC low-x and low-Q^2 data.

Keywords Particular solution, complete solution, Alterelli-Parisi equation, structure function

PACS Nos. . 12.38.Bx, 12 39.-x, 13.60.Hb

1. Introduction

The Gribov-Lipatov-Dokshitzer-Altarelli-Parisi (GLDAP) evolution equations[1-4] are fundamental tools to study the $t\left(=\ln(Q^2/\Lambda^2)\right)$ and x- evolutions of structure functions, where x and Q^2 are Bjorken scaling and four momenta transfer in a deep inelastic scattering (DIS) Process [5] respectively and Λ is the QCD cut-off parameter. On the other hand, the study of structure functions at low-x has become topical in view [6] of high energy collider and supercollider experiments [7]. Solutions of GLDAP evolution equations give quark and gluon structure functions which produce ultimately proton, neutron and deuteron structure functions. Though numerical solutions are available in the literature [8], the explorations of the possibility of obtaining analytical solutions of GLDAP evolution equations are always interesting. In this connection, some particular solutions computed from general solutions of GLDAP evolution equations at low-x in leading order have already been obtained by applying Taylor expansion method [9] and t-evolutions [10] and x- evolutions [11] of structure functions have been presented.

The present paper reports particular solutions of GLDAP evolution equations computed from complete solutions in leading order at low-x and calculation of t and x-evolutions for singlet and non-singlet structure functions and hence t-evolutions of proton and neutron structure functions and x-evolutions of deuteron structure functions. In some instance, we can deal with particular solutions more conveniently than with the general solutions [12]. In calculating structure functions, input data points have been taken from the experimental data directly, unlike the usual practice of using an input distribution function introduced arbitrarily. Results of proton and neutron structure functions are compared with the HERA low-x low-Q^2 data and those of deuteron structure functions are compared with the NMC low-x low-Q^2 data. Comparisons are also made with the results of earlier solutions [10, 11, 13] of GLDAP evolution equations. In Section 2, necessary theory has been discussed. Section 3 gives results and discussion.

2. Theory

Though the basic theory has been discussed elsewhere [10, 11, 13], the essential steps of the theory have been presented here for clarity. The GLDAP evolution equations for singlet and non-singlet structure functions in the standard forms are [14] :

$$\frac{\partial F_2^S(x,t)}{\partial t} - \frac{A_f}{t}\left[\{3+4\ln(1-x)\}\, F_2^S(x,t) + I_1^S(x,t) + I_2^S(x,t)\right] = 0 \quad (1)$$

* Corresponding Author

and

$$\frac{\partial F_2^{NS}(x,t)}{\partial t} - \frac{A_f}{t}\left[\{3+4\ln(1-x)\}\, F_2^{NS}(x,t) + I^{NS}(x,t)\right] = 0, \quad (2)$$

where,

$$I_1^S(x,t) = 2\int_x^1 \frac{dw}{1-w}\left\{\left(1+w^2\right)F_2^S(x/w,t) - 2F_2^S(x,t)\right\}, \quad (3)$$

$$I_2^S(x,t) = \frac{3}{2} N_f \int_x^1 \left\{w^2 + (1-w)^2\right\} G(x/w,t)\, dw, \quad (4)$$

and

$$I^{NS}(x,t) = 2\int_x^1 \frac{dw}{1-w}\left\{\left(1+w^2\right) F_2^{NS}(x/w,t) - 2F_2^{NS}(x,t)\right\}. \quad (5)$$

Here, $t = \ln\left\{Q^2/\Lambda^2\right\}$ and $A_f = 4/(33-2N_f)$, N_f being the number of flavours and Λ is the QCD cut off parameter.

Let us introduce the variable $u = 1-w$ and note that [15]

$$\frac{x}{w}\quad\frac{x}{1-u} = x\sum_{k=0}^{\infty} u^k. \quad (6)$$

The series (6) is convergent for $|u| < 1$. Since $x < w < 1$, so $0 < u < 1-x$ and hence the convergence criterion is satisfied. Now, using Taylor expansion method [9], we can rewrite $G(x/w, t)$ as

$$G(x/w,t) = G\left(x + x\sum_{k=1}^{\infty} u^k, t\right)$$

$$= G(x,t) + x\sum_{k=1}^{\infty} u^k \frac{\partial G(x,t)}{\partial x} + \frac{1}{2}x^2\left(\sum_{k=1}^{\infty} u^k\right)^2 \frac{\delta^2 G(x,t)}{\partial x^2} + \ldots \quad (7)$$

which covers the whole range of u, $0 < u < 1-x$. Since x is small in our region of discussion, the terms containing x^2 and higher powers of x can be neglected as the first approximation as discussed in our earlier works [11, 12, 14] and $G(x/w, t)$ can be approximated for small-x as

$$G(x/w,t) \cong G(x,t) + x\sum_{k=1}^{\infty} u^k \frac{\partial G(x,t)}{\partial x} \quad (8)$$

Similarly, $F_2^S(x/w,t)$ and $F_2^{NS}(x/w,t)$ can be approximated for small-x as

$$F_2^S(x/w,t) \cong F_2^S(x,t) + x\sum_{k=1}^{\infty} u^k \frac{\partial F_2^S(x,t)}{\partial x}, \quad (9)$$

and

$$F_2^{NS}(x/w,t) \cong F_2^{NS}(x,t) + x\sum_{k=1}^{\infty} u^k \frac{\partial F_2^{NS}(x,t)}{\partial x}. \quad (10)$$

Using eqs. (8)-(10) in eqs. (3)-(5) and performing u-integrations, we get

$$I_1^S = -\left[(1-x)(x+3)\right] F_2^S(x,t) + \left[2x\ln(1/x) + x\left(1-x^2\right)\right] \frac{\partial F_2^S(x,t)}{\partial x} \quad (11)$$

$$I_2^S = N_f\left[\frac{1}{2}(1-x)\left(2-x+2x^2\right)G(x,t) + \left\{-\frac{1}{2}x(1-x)\left(5-4x+2x^2\right) + \frac{3}{2}x\ln(1/x)\right\}\frac{\partial G(x,t)}{\partial x}\right] \quad (12)$$

and

$$I^{NS} = -\left[(1-x)(x+3)\right] F_2^{NS}(x,t) + \left[2x\ln(1/x) + x\left(1-x^2\right)\right]\frac{\partial F_2^{NS}(x,t)}{\partial x}.$$

Now using eqs. (11) and (12) in eq. (1), we have

$$\frac{\partial F_2^S(x,t)}{\partial t} - \frac{A_f}{t}\left[A(x)F_2^S(x,t) + B(x)\frac{\partial F_2^S(x,t)}{\partial x} + C(x)\, G(x,t) + D(x)\frac{\partial G(x,t)}{\partial x}\right] = 0.$$

Let us assume for simplicity

$$G(x,t) = K(x)\, F_2^S(x,t), \quad (15)$$

where $K(x)$ is a function of x. Now, eq. (14) gives

$$\frac{\partial F_2^S(x,t)}{\partial t} - \frac{A_f}{t}\left[L(x)\, F_2^S(x,T) + M(x)\frac{\partial F_2^S(x,t)}{\partial x}\right] = 0, \quad (16)$$

where

$$A(x) = 3 + 4\ln(1-x) - (1-x)(3+x),$$

$$B(x) = x(1-x^2) + 2x\ln(1/x),$$

$$C(x) = 1/2N_f(1-x)(2-x+2x^2),$$

$$D(x) = N_f x\left[-\frac{1}{2}(1-x)\left(5-4x+2x^2\right) + \left(\frac{3}{2}\right)\ln\left(\frac{1}{x}\right)\right]$$

$$L(x) = A(x) + K(x)C(x) + D(x)\frac{\partial K(x)}{\partial x}$$

and $M(x) = B(x) + K(x)\, D(x)$.

Secondly, using eq. (13) in eq. (2), we have

$$\frac{\partial F_2^{NS}(x,t)}{\partial t} - \frac{A_f}{t}\left[P(x)\, F_2^{NS}(x,t) + Q(x)\frac{\partial F_2^{NS}(x,t)}{\partial x}\right] = 0, \quad (17)$$

where

$$P(x) = 3 + 4\ln(1-x) - (1-x)(x+3),$$

and

$$Q(x) = x(1-x^2) - 2x\ln x .$$

The general solutions of eqs. (16) is [9, 12] $F(U, V) = 0$, where F is an arbitrary function and

$$U\left(x, t, F_2^S\right) = C_1$$

and

$$V\left(x, t, F_2^S\right) = C_2$$

form a solution of equation

$$\frac{dx}{A_f M(x)} \quad \frac{dt}{-t} \quad \frac{dF_2^S(x,t)}{-A_f L(x) F_2^S(x,t)} \tag{18}$$

Solving eq. (18) we obtain,

$$U\left(x, t, F_2^S\right) = t \exp\left[\frac{1}{A_f}\int \frac{1}{M(x)}dx\right]$$

and

$$V\left(x, t, F_2^S\right) = F_2^S(x,t)\exp\left[\int \frac{L(x)}{M(x)}dx\right]$$

If U and V are two independent solutions of eq. (18) and if α and β are arbitrary constants, then $V = \alpha U + \beta$ may be taken as a complete solution of eq. (18). We take this form as this is the simplest form of a complete solution which contains both the arbitrary constants α and β. Earlier [10, 11, 13], we considered a solution $AU + BV = 0$, where A and B are arbitrary constants. But that is not a complete solution having both the arbitrary constants as this equation can be transformed to the form $V = CU$, where $C = -A/B$, *i.e.* the equation contains only one arbitrary constant.

Now, the complete solution [9, 12]

$$F_2^S(x,t)\exp\left[\int \frac{L(x)}{M(x)}dx\right] = \alpha t \exp\left[\frac{1}{A_f}\int \frac{1}{M(x)}dx\right] + \beta \tag{19}$$

is a two-parameter family of surfaces, which does not have an envelope, since the arbitrary constants enter linearly [9]. Differentiating eq. (19) with respect to β, we get $0 = 1$ which is absurd. Hence, there is no singular solution. The one-parameter family determined by taking $\beta = \alpha^2$ has equation

$$F_2^S(x,t)\exp\left[\int \frac{L(x)}{M(x)}dx\right] = \alpha t \exp\left[\frac{1}{A_f}\int \frac{1}{M(x)}dx\right] + \alpha^2 . \tag{20}$$

Differentiating eq. (20) with respect to α, we get

$$\alpha = -\frac{1}{2}t \exp\left[\frac{1}{A_f}\int \frac{1}{M(x)}dx\right]$$

Putting the value of α in eq. (20), we obtain the envelope

$$F_2^S(x,t) = -\frac{1}{4}t^2 \exp\left[\frac{1}{A_f M(x)} - \frac{L(x)}{M(x)}\right]dx \tag{21}$$

which is merely a particular solution of the general solution. Unlike the case of ordinary differential equations, the envelope is not a new locus. It is to be noted that when β is an arbitrary function of α, then the elimination of α in eq. (20) is not possible. Thus, the general solution can not be obtained from the complete solution [9]. Actually, the general solution of a linear partial differential equation of order one is the totality of envelopes of all one-parameter families (21) obtained from a complete solution.

Now, defining

$$F_2^S(x_0, t) = -\frac{1}{4}t_0^2 \exp\left[\frac{1}{A_f M(x)} - \frac{L(x)}{M(x)}\right]dx\Bigg],$$

at $t = t_0$, where $t_0 = \ln\left(Q_0^2/\Lambda^2\right)$ at any lower value $Q = Q_0$, we get from eq. (21)

$$F_2^S(x,t) = F_2^S(x_0,t)\left(\frac{t}{\cdot}\right)^{\cdot}, \tag{22}$$

which gives the t-evolution of singlet structure function $F_2^S(x, t)$.

Proceeding exactly in the same way, and defining

$$F_2^{NS}(x, t_0) = -\frac{1}{4}t_0^2 \exp\int\left(\frac{2}{A_f Q(x)} - \frac{P(x)}{Q(x)}\right)dx$$

we get for non-singlet structure function

$$F_2^{NS}(x,t) = F_2^{NS}(x,t_0)\left(\frac{t}{\cdot}\right)^{\cdot}, \tag{23}$$

which gives the t-evolution of non-singlet structure function $F_2^{NS}(x, t)$.

Again defining

$$F_2^S(x_0,t) = -\frac{1}{4}t^2 \exp\left[\frac{1}{A_f M(x)} - \frac{L(x)}{M(x)}\right]dx$$

we obtain from eq. (21)

$$F_2^S(x,t) = F_2^S(x_0,t)\exp\int_{x_0}^{x}\left(\frac{2}{A_f M(x)} - \frac{L(x)}{M(x)}\right)dx \tag{24}$$

respectively, with the HERA low-x, low-Q^2 data [16]. Here, proton structure functions $F_2^p(x, Q^2, z)$ measured in the range $2 \le Q^2 \le 50$ GeV^2, $0.73 \le z \le 0.88$ and neutron structure functions $F_2^n(x, Q^2, z)$ measured in the range $2 \le Q^2 \le 50$ GeV^2, $0.3 \le z \le 0.9$ have been used. Moreover, here $P_T \le$ 200MeV, where P_T is the transverse momentum of the final state baryon and $z = 1-q.(p-p')/(q.p)$, where p, q are the four momenta of the incident proton and the exchanged vector boson coupling to the positron and p' is the four-momentum of the final state baryon. Though we compare our results with $y = 2$ in $\beta = \alpha^y$ relation with data, our results with y maximum, which are equivalent to our earlier results are equally valid. For t-evolutions of deuteron, proton and neutron structure functions, the results will be the range-bounded by our new and old results. But for x-evolutions of deuteron structure function, new and old results have not any significance difference.

In Figure 1, we present our results of t-evolutions of proton structure functions F_2^p (solid lines) for the representative values of x given in the figure. Data points at lowest-Q^2 values in the figure are taken as input to test the evolution equation (33). Agreement is found to be excellent. In the same figure, we also plot the results of t-evolutions of proton structure functions F_2^p (dashed lines) for our earlier solutions from eq. (35) of GLDAP evolution equations. We observe that our new results are in better agreement with data than the old ones.

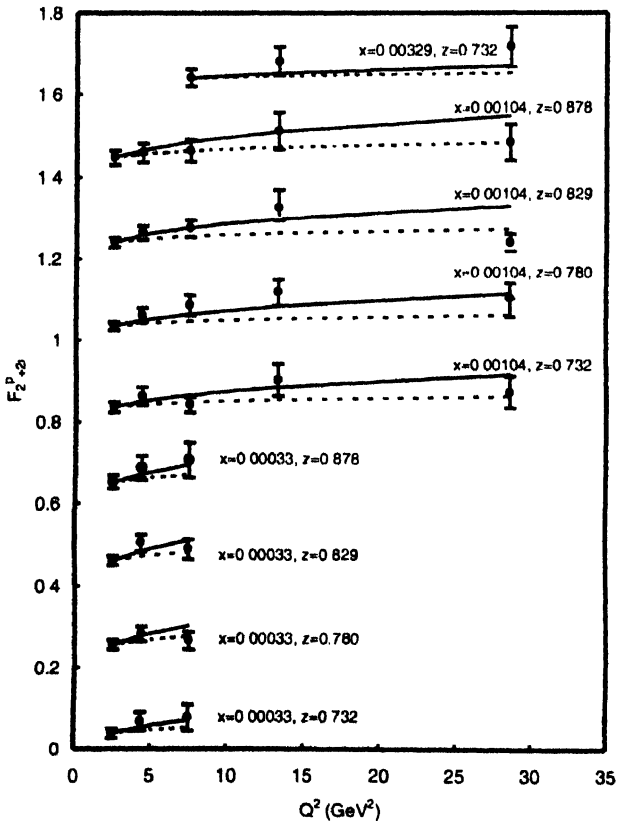

Figure 1. t-evolutions of proton structure functions F_2^p (solid lines) for the representative values of x. Data points at lowest-Q^2 values are taken as input to test the evolution equation (33). We also plot the results of t-evolutions of proton structure functions F_2^p (dashed lines) for our earlier solutions from eq. (35) of GLDAP evolution equations. For convenience, value of each data point is increased by adding $0.2i$, where i = 0,1,2,3,... are the numberings of curves counting from the bottom of the lowermost curve as the 0-th order.

In Figure 2, we present our results of t-evolutions of neutron structure functions F_2^n (solid lines) for the representative values of x given in the figure. Data points at lowest- Q^2 values in the figure are taken as input to test the evolution eq. (34). Agreement is found to be excellent. In the same figure, we also plot the results of t-evolutions of neutron structure functions F_2^n (dashed lines) for our earlier solutions from eq. (36) of GLDAP evolution equations. We observe that in this case also, our new results are in better agreement with data than the old ones.

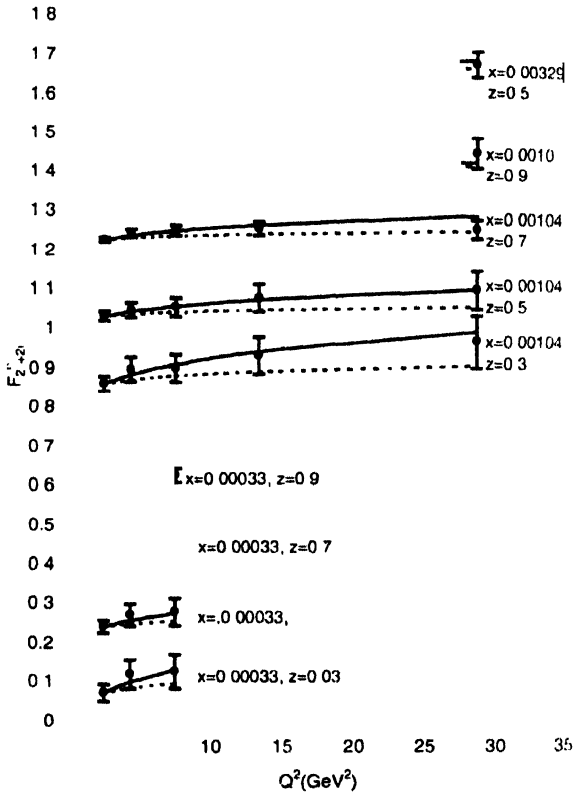

Figure 2. t-evolutions of proton structure functions F_2^n (solid lines) for the representative values of x. Data points at lowest-Q^2 values are taken as input to test the evolution equation (34). We also plot the results of t evolutions of neutron structure functions F_2^n (dashed lines) for our earlier solutions from eq. (36) of GLDAP evolution equations. For convenience value of each data point is increased by adding $0.2i$, where i = 0, 1, 2, 3 are the numberings of curves counting from the bottom of the lowermost curve as the 0-th order.

For a quantitative analysis of x-distributions of structure functions, we calculate the integrals that occurred in eq. (30) for $N_f = 4$. In Figure 3, we present our results of x-distribution of deuteron structure functions F_2^d for $K(x)$ = constant (solid lines), $K(x) = ax^b$ (dashed lines) and for $K(x) = ce^{-dx}$ (dotted lines), where a, b, c and d are constants and for representative values of Q^2 given in each figure, and compare them with NMC deuteron low-x low- Q^2 data[17]. In each, the data point for x- value just below 0.1 has been taken as input F_2^d (x_0, t).

If we take $K(x) = 4.5$ in eq. (30), then agreement of the result with experimental data is found to be excellent. On the other hand, if we take $K(x) = ax^b$, then agreement of the results with experimental data is found to be good at $a = 4.5, b = 0.01$. Again if we take $K(x) = ce^{-dx}$, then agreement of the results with experimental data is found to be good at $c = 5, b = 1$.

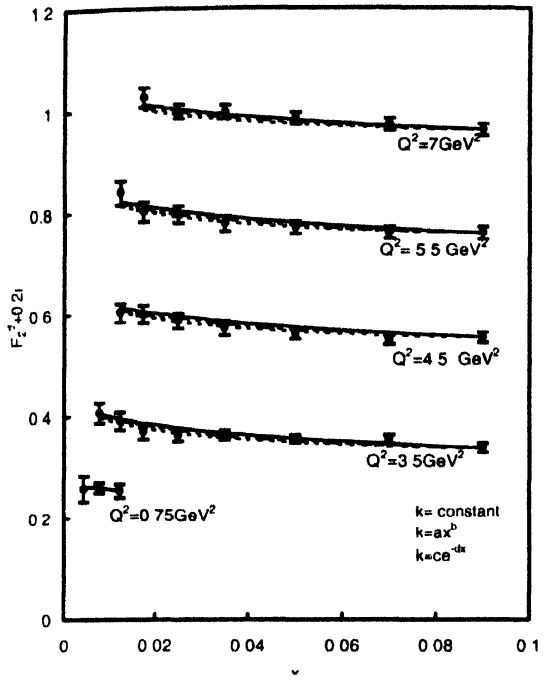

Figure 3. x distributions of deuteron structure functions F_2^d for $K(x)$ = constant (solid lines), $K(x) = ax^b$ (dashed lines) and for $k(x) = ce^{-dx}$ (dotted lines), where a, b, c and d are constants, and compare them with NMC deuteron low-x low-Q^2 data. In each, the data point for x- value just below 0 1 has been taken as input $F_2^d(x_0, t)$. For convenience, value of each data point is increased by adding $0.2i$, where i = 0, 1, 2, 3, ... are the numberings of curves counting from the bottom of the lowermost curve as the 0-th order.

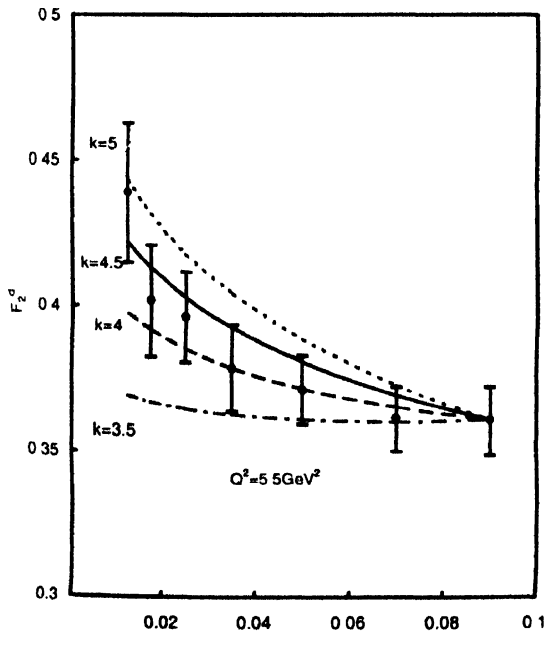

Figure 4. Sensitivity of our results for different constant values of $K(x)$.

In Figure 4, we present the sensitivity of our results for different constant values of $K(x)$, we observe that at $K(x) = 4.5$, agreement of the results with experimental data is found to be excellent. If value of $K(x)$ is increased, the curve goes upward direction and if value of $K(x)$ is decreased, the curve goes downward direction. But the nature of the curve is similar.

In Figure 5, we present the sensitivity of our results for different values of a at fixed value of b. Here, we take $b = 0.01$. We observe that at $a = 4.5$, agreement of the results with experimental data is found to be excellent. If value of a is increased, the curve moves upward and if value of a is decreased, the curve goes downward. But the nature of the curve is similar.

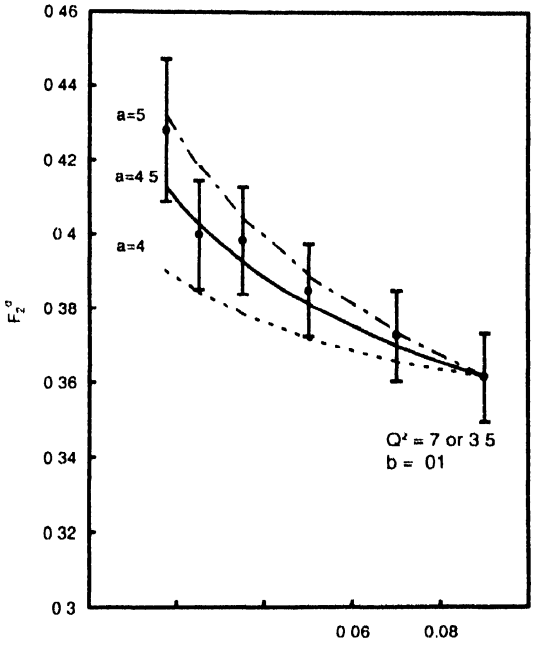

Figure 5. Sensitivity of our results for different values of a at fixed value of b = 0 01

In Figure 6, we present the sensitivity of our results for different values of b at fixed value of a. Here, we take $a = 4.5$, we observe that at $b = 0.01$, agreement of the results with experimental data is excellent. If value of b is increased, then the curve goes downward and if value of b is decreased, the curve goes upward. But we observe that difference of the curves for $b = 0.01, 0.001, 0.0001$ is very small and all these curves are overlapped. Here also the nature of the curves is similar.

In Figure 7, we present the sensitivity of our results for different values of 'c' at fixed value of 'd'. Here, we take $d = 1$. We observe that at $c = 5$, agreement of the results with experimental data is excellent. If value of 'c' is increased, the curve goes upward and if value of 'c' is decreased, the curve goes downward direction. But the nature of the curves is similar.

In Figure 8, we present sensitivity of our results for different values of d at fixed value of c. Here, we take $c = 5$, we observe that at $d = 1$, agreement of the results with experimental data is excellent. If value of 'd' is increased, then the curve goes